Self-Assembled Hydrogel Nanoparticles Responsive to Tumor Extracellular pH from Pullulan Derivative/Sulfonamide Conjugate: Characterization, Aggregation, and Adriamycin Release *in Vitro*

Kun Na[1] and You Han Bae[1,2]

Received December 20, 2001; accepted January 4, 2002

Purpose. To investigate some physicochemical properties of self-assembled hydrogel nanoparticles of pullulan acetate (PA) and sulfonamide conjugates, as a potential tumor targeting drug carrier responsive to tumor extracellular pH.

Methods. A new class of pH-responsive polymers was synthesized by conjugating a sulfonamide, sulfadimethoxine (SDM), to succinylated pullulan acetate (coohPA). The polymers formed self-assembled PA/SDM hydrogel nanoparticles in aqueous media, which was confirmed by fluorometry and field emission-scanning electron microscopy. The pH-dependent behavior of the nanoparticles was examined by measuring transmittance, particle size and zeta potential. Adriamycin (ADR) was tested for loading into and release from the nanoparticles at various pHs.

Results. The mean diameters of all PA/SDM nanoparticles tested were <70 nm, with a unimodal size distribution. The critical aggregation concentrations at pH 9.0 were as low as 3.16 μg/mL. The nanoparticles showed good stability at pH 7.4, but shrank and aggregated below pH 7.0. The ADR release rate from the PA/SDM nanoparticles was pH-dependent around physiological pH and significantly enhanced below a pH of 6.8.

Conclusions. The pH-responsive PA/SDM nanoparticles may provide some advantages for targeted anti-cancer drug delivery due to the particle aggregation and enhanced drug release rates at tumor pH.

KEY WORDS: sulfonamide; pullulan acetate; self-assembled hydrogel nanoparticles; anti-cancer drug delivery; adriamycin; tumor pH.

INTRODUCTION

Most cytostatic agents are not as effective in cancer chemotherapy as anticipated because of nonspecific toxicity, lacking tumor selectivity, and development of multidrug resistance in various tumor cells. The passive accumulation of various colloidal nanocarriers with optimum sizes, such as liposomes and polymeric nanoparticles or micelles, in solid tumor sites by a process termed "enhanced permeation and retention (EPR)," has prompted an extensive investigation of these systems for effective anti-cancer drug delivery (1–3). In addition, a more efficient delivery mode of anti-cancer drug, which switches from a slow-release rate in the systemic circulation to a fast-release at the tumor site, is anticipated (2).

Polymeric nanoparticles constructed from stimuli-sensitive polymers have been proposed as new anti-cancer drug carriers. Such polymeric nanoparticles alter their physical properties, such as swelling/deswelling, particle disruption and/or aggregation, in response to the changes in environmental condition. These features may alter the interactions of the nanoparticles with cells and switches the carriers system from slow to fast drug release. There have been recent reports for the possibility of developing thermo-sensitive polymeric nanoparticles for the double-targeting of anticancer drugs to tumors, i.e., passive accumulation/aggregation and the enhanced release of loaded drugs by an externally provided hyperthermic condition (4–6).

One of the consistent differences between various solid tumors and the surrounding normal tissue is the nutritional and metabolic environment. The vasculature of tumors is often insufficient to supply enough oxygen and nutritional needs for the expanding population of tumor cells. The production of lactic acid under hypoxic conditions and the hydrolysis of ATP in an energy-deficient environment contribute to an acidic micro-environment, which has been found in many types of tumors. Most solid tumors have lower extracelluar pH (pH_e) (<7.2) than the surrounding tissues and blood (pH 7.5) (7,8).

It has been proposed that pH-induced anticancer drug release from pH-sensitive liposomes based on carboxylic group, stable at neutral pH but leaky under mildly acidic condition (pH 4.5–6.0) (9–10), could be a new mode of cancer treatments. However due to the lack of responsive property to the range of tumor acidity (pH 6.5–7.2), these carriers limit their utility as tumor targeting. Leroux *et al.* discussed that the pH_e rarely declines below pH 6.5 and thus makes it technically difficult to engineer liposomes that become disrupted in such a narrow window of pH (11). More recently, pH-sensitive nanocarriers have been more justified as cytosolic drug delivery carriers, instead of targeting to tumor pH_e, via endocytosis mechanism to improve drug bioavailability because endosomes and lysosomes are more acidified by proton-translocating ATPase to an average pH of approximately 5.0 (12–15). Thus it is necessary to develop a nanocarriers which are truly responsive to tumor pH_e for direct tumor targeting.

To acquire the appropriate pH-sensitivity, self-assembled hydrogel nanoparticles were prepared by introducing sulfadimethoxine (SDM, pKa; 6.1) into pullulan acetate (PA) (Fig. 1). Pullulan, is a linear polysaccharide with an α-(1-6)-linked maltotriosyl repeating unit, and is now commercially available. A number of pullulan derivatives have been prepared to investigate their potential applications in pharmaceutical and biomedical fields (16,17). SDM is a member of the sulfonamide family and has been used as an antibacterial agent (18). Sulfonamide is a weak acid because the hydrogen atom of sulfonamide nitrogen can be readily ionized to liberate a proton in solution. Our previous paper

[1] Center for Biomaterial and Biotechnology, Department of Materials Science and Engineering, Kwangju Institute of Science and Technology, 1 Oryong-Dong, Puk-gu, Kwangju 500-712, Korea.

[2] To whom correspondence should be addressed. (e-mail: yhbae@kjist.ac.kr)

ABBREVIATIONS: PA, pullulan acetate; SDM, sulfadimethoxine; DS, degree of substitution, defined as the number of substitution per anhydroglucose unit; PA/SDM, pullulan acetate and sulfadimethoxine conjugate; ADR, adriamycin; CAC, critical aggregation concentrations; DLS, dynamic light scattering; FE-SEM, field emission-scanning electronic microscopy.

0724-8741/02/0500-0681/0 © 2002 Plenum Publishing Corporation

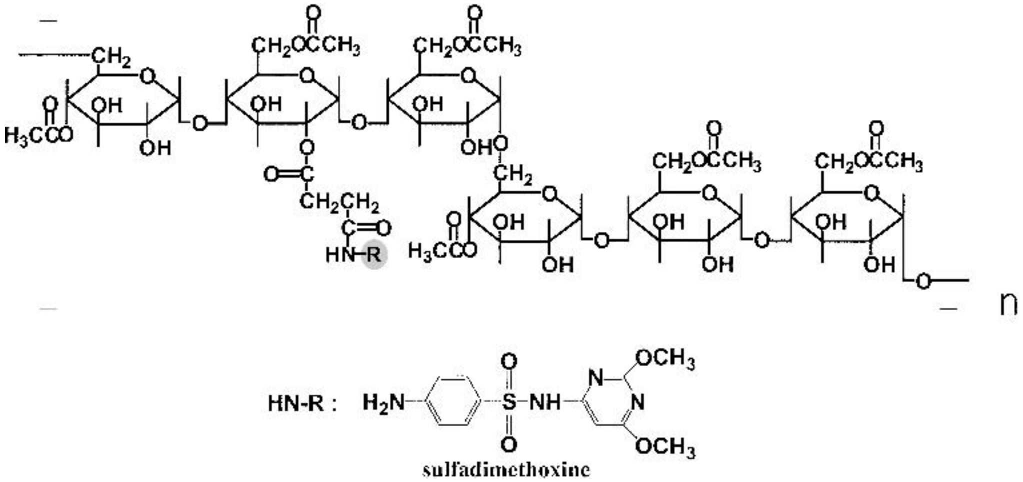

Fig. 1. Chemical structure of pullulan acetate (PA)/sulfadimethoxine (SDM) conjugate.

reported that copolymers synthesized from a monomeric derivative of sulfamethazine and *N,N*-dimethylacrylamide showed reversible solubility around physiological pHs (19).

In this paper, we report some physicochemical properties of PA/SDM nanoparticles in terms of particle size, critical aggregation concentration (CAC) and stability in aqueous media. We also examined the aggregation behavior of PA/SDM nanoparticles as a function of pH and the release kinetics of a model drug, adriamycin, to explore the possibility of the new polymeric system as an anti-cancer drug carrier.

MATERIALS AND METHODS

Materials

Pullulan (Mw 200,000) was obtained from Hayashibara, Japan. Acetic anhydride, succinic anhydride, sulfadimethoxine [4-amino-N-(2,6-dimethoxy-4-pyrimidynyl)benzenesulfonamide] (SDM), dicyclohexyl carbodiimide (DCC), N-hydroxysuccinimide (HOSU), and 4-dimethylaminopyridine (DMAP) were purchased from Sigma, St. Louis, Missouri. Adriamycin (ADR) was kindly supplied by Boryung Pharm. Co. Ltd. (Ansan, Korea). All other chemicals used were of reagent grade.

Pullulan Acetylation

To impart the amphiphilicity, pullulan was chemically modified by acetylation. Pullulan (2 g) was suspended in 20 mL of formamide and dissolved by vigorous stirring at 50°C. Pyridine (60 mL) and acetic anhydride (150 mL) were added and the mixture was stirred at 54°C for 48 h. Pullulan acetate (PA) was obtained by precipitation from 200 mL of water. The synthesized PA was identified using FT-IR and NMR spectrophotometers. The NMR result gave the degree of acetylation, 1.17 acetyl groups per glucose unit of pullulan.

Synthesis of PA/SDM Conjugate

To conjugate PA and SDM, PA was first succinylated using succinic anhydride. PA (5.0 g) was dissolved in 200 mL of 1,4-dioxane purified by vacuum distillation. Succinic anhydride (2.2 g) and 4-dimethylaminopyridine (DMAP; 2.0 g) and triethyl amine (1.8 g) as catalysts were added. The reaction mixture was stirred for 24 h at room temperature. This procedure was carried out in a nitrogen atmosphere. After reaction, 1,4-dioxane was removed using a rotary evaporator and the product was dissolved in 300 mL of carbon tetrachloride to remove unreacted succinic anhydride. The solution was filtered, and the filtrate concentrated to 100–150 mL using the rotar evaporator and precipitated in cold diethyl ether (4°C). The degree of succinylation was 0.54 carboxyl groups per glucose unit of PA, as determined by ^{1}H-NMR and gel permeation chromatography (GPC).

SDM was coupled to the succinylated PA (coohPA) via amide linkage using a dicyclohexyl carbodiimide (DCC) and N-hydroxylsuccinimide (HOSU)-mediated reaction. Different amounts of SDM (300, 700 mg), DCC (250, 500 mg) and HOSU (150, 350 mg) were added to 40 mL of dry DMSO containing 1 g of coohPA and reacted for 24 h at room temperature. Precipitated dicyclohexylurea (DCU) was removed by filtration. After 24 h, the reactant mixtures were filtered and dialyzed using a dialysis tube (molecular cutoff 12,000) against distilled water for 3 days. The samples were then lyophilized. The lyophilized product was purified by dissolution in DMSO and re-dialyzing against distilled water; this process was repeated three times. The PA/SDM conjugates obtained were characterized by IR (Perkin-Elmer 2000 series IR, KBr pellet), ^{1}H-NMR (JEOL JNM-LA 300 WB FT-NMR) and GPC [Waters LC system coupled to a Waters 410 Differential Refrectometer using Styragel™ HR Series column at a flow rate of 1 mL/min. Eluent; tetrahydrofuran (THF)]. In the NMR measurement, all samples were dissolved in DMSO-d_6 (Aldrich) and tetramethylsilane (TMS; Aldrich) was used as a reference. The degree of substitution (DS), was defined as the number of SDM groups per anhydroglucose unit of the pullulan acetate, and was determined by ^{1}H-NMR. The DS of two PA/SDMs produced were 0.17 (PA/SDM 1) and 0.39 (PA/SDM 2), respectively.

Preparation of Self-Assembled Nanoparticles from PA and PA/SDM

The polymers were self-assembled into hydrogel nanoparticles using a diafiltration method (molecule cut-off of dialysis tubing: 2000). Amphiphiles (50 mg) were dissolved in 20 mL of DMSO. Each polymer solution was dialyzed against borate buffer (NaOH, $Na_2B_4O_7$; pH 9.0) at room temperature for two days. The solution was filtered through a 0.45 μm filter to remove precipitated materials.

Particle Size Measurement

The particle size of the resulting nanoparticles was determined by dynamic light scattering (DLS, Malvern Instruments Ltd. Series 4700, Malvern, United Kingdom). The DLS experiment was performed with an argon ion laser system tuned at a wavelength of 488 nm. Each sample was filtered through a 0.45-μm filter directly into a precleaned 10 mm diameter cylindrical cell. Intensity autocorrelation was measured at a scattering angle (θ) of 90 degree at 25°C. The sample concentration was maintained at 1.0 mg/mL.

Measurement of Fluorescence Spectroscopy (Pyrene)

A stock solution of pyrene (6.0×10^{-2} M) was prepared in acetone and stored at 5°C. To obtain the steady-state fluorescence spectra, the pyrene solution was diluted with distilled water to a pyrene concentration of 12.0×10^{-7} M. The solution was then distilled under vacuum at 60°C for 1 h to remove the acetone. The acetone-free pyrene solution was then mixed with nanoparticle suspensions, of which concentration ranged from 1×10^{-4} to 1.0 mg/mL. The final concentration of pyrene in each sample was 6.0×10^{-7} M.

Light Transmittance of Nanoparticle Solution

The optical transmittance of the nanoparticle solution (1 g/L) at various pHs was measured at 500 nm using Varian CARY 1E UV/Vis spectrometer. The pH was gradually lowered by adding 0.01 N HCl solution, and the relative transmittances (%) at differing pH were expressed relative to the transmittance at pH 9.0 (100%).

Zeta Potential Measurement of the PA/SDM Nanoparticles

The average zeta potential of the nanoparticles was determined as a function of pH using a zeta potentiometer (Zetasizer 3000, Malvern Instruments Ltd, Malvern, United Kingdom). An electric field of 150 V was applied to observe the electrophoretic mobility of the nanoparticles. The zeta potential was determined by varying the pH at a fixed particle concentration of 1 g/L.

Morphological Observations of the PA/SDM Nanoparticles

The morphologies of the nanoparticles were observed under a FE-SEM (S-4700, Hitachi, Ibaraki, Japan). A drop of the hydrogel nanoparticles in water was placed on a graphite surface and coated with Pt by sputtering, for 4 min at 20 mA.

ADR Loading and Release

ADR·HCl (20 mg) and 1.3 equivalents of triethylamine were reacted in N,N-dimethyl acetamide (DMAc) (3ml) to form ADR basic adduct. The pullulan derivative (50 mg, coohPA or PA/SDM) was added to the ADR solution and the mixture was stirred overnight at 4°C in a dark condition. The polymer/ADR solution was transferred into a dialysis tubing (Spectra /Por molecular weight cut-off size 15,000) and then dialyzed against borate buffer solution for three days at 25°C. The buffer was exchanged with a fresh solution every 3 h for the first 24 h, and then daily. The solution was filtered through a 0.45-μm filter to remove precipitated polymer and drug, and freeze-dried to obtain ADR loaded hydrogel nanoparticles. To determine drug-loading content, a freeze-dried sample was placed in DMAc, vigorously stirred for 2 h and then sonicated for 3 min. The resulting solution was centrifuged at 20,000 g for 30 min and the supernatant was analyzed using a UV spectrophotometer at 490 nm.

The release rate measurement *in vitro* was carried out as follows: 2 mL of drug-loaded PA/SDM nanoparticles solution (1 g/L in a dialysis tube) was placed in 10 mL of phosphate buffered saline (PBS) at various pHs (6.0, 6.8, 7.4, and 8.0). The release medium was stirred at 100 rpm and 37°C. At predetermined sampling times, the whole medium was removed and replaced by fresh PBS to maintain a sink conditions. The amount of ADR in the solution was determined by UV-spectroscopy at 490 nm.

RESULTS AND DISCUSSION

Physicochemical Properties of PA/SDM Nanoparticles

PA/SDM polymers with two different degrees of SDM substitution (DS = 0.17 and 0.39) were synthesized. Self-assembled nanoparticles were then prepared by the diafiltration method, which prevented the uncontrolled rapid precipitation of the polymer during the self-assembly process. The size and size distribution of the nanoparticles were measured by DLS. The results revealed that the size of the nanoparticles prepared from all polymers except PA was less than 70 nm,

Table I. Properties and Drug Loading Efficiency of Self-Assembled Hydrogel Nanoparticles in Aqueous Media (pH 9.0)

Sample	DS	Particle size[b] ± SD (nm)	CAC[c] × 10^3 (mg/mL)	ADR loading efficiency[d] ± SD (%)
PA	1.17[a-1]	118 ± 55	1.07	28 ± 5.5
CoohPA	0.44[a-2]	51 ± 24	8.55	18 ± 5.6
PA/SDM 1	0.17[a-3]	56 ± 22	5.04	24 ± 2.4
PA/SDM 2	0.39[a-3]	61 ± 29	3.16	25 ± 3.2

[a-1 and 2] Degree of substitution of acetyl and carboxymethyl groups per anhydroglucose unit of pullulan. [a-3]Degree of substitution of SDM per anhydroglucose unit of pullulan, (using NMR and GPC).

[b] Mean diameter (intensity average) measured by dynamic light scattering.

[c] Critical aggregation concentration determined from I_{337}/I_{334} data.

[d] Drug loading efficiency was calculated as loaded drug weight/initial drug weight × 100.

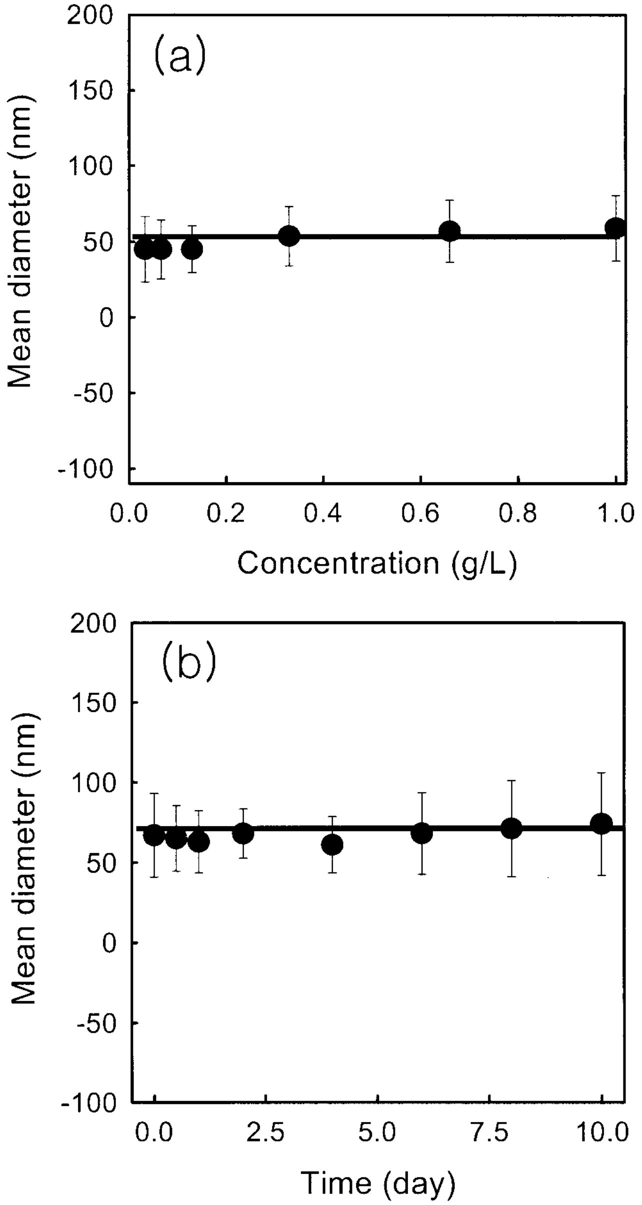

Fig. 2. Size changes of PA/SDM 2 nanoparticles as functions of nanoparticle concentration (a) and time (b) at pH 7.4 (1 g/L).

which is equivalent to those of viruses or lipoproteins and smaller than the critical size (about 100 nm) required for the recognition by reticuloendothelial systems (RES) (20) (Table I). The self-assembling process of a PA/SDM polymer in aqueous media was monitored by pyrene study. At low concentrations of PA/SDM 1, the change in total fluorescence intensity and the shift of the (0,0) band at 334 nm are negligible. As the PA/SDM 1 concentration was increased, however, an increase in the total fluorescence intensity and a red shift of the (0,0) band were observed, indicating that pyrene is transferred from the aqueous media to the less polar microdomains (interior) of the nanoparticles. The (0,0) band for pyrene at 334 nm shifts to 337 nm on adding PA/SDM 1 (data not shown). The critical aggregation concentration (CAC), which is the threshold concentration of the polymer required to form self-assembled nanoparticles by intra- and/or intermolecular association, was determined from the change in the intensity ratio (I_{337}/I_{334}) of the pyrene in presence of the polymer. The CACs of self-assembled nanoparticles at pH 9.0 are listed in Table I. The determined CACs were lower than the typical critical micelle concentration (CMC) of low-molecular-weight surfactants, such as sodium dodecyl sulfate and deoxycholic acid in water. The lower CAC values of PA derivatives may be one of the important characteristics of the polymeric amphiphiles examined in this study; suggests micelle stability in a dilute condition.

To investigate the stability of PA/SDM nanoparticles formed at pH 9.0, we measured the particle size as function of the nanoparticle concentration and time at pH 7.4. Fig. 2(a) shows that the size of PA/SDM 2 nanoparticles at pH 7.4 was unaffected by decreasing nanoparticle concentration. Moreover, the mean particle diameter remained almost unchanged on diluting to 0.03 g/L. This result suggests negligible interparticle interactions and the high stability of self-assembled nanoparticles. Fig. 2(b) shows the change of PA/SDM 2 nanoparticles over time at a fixed nanoparticle concentration of 1g/L. The nanoparticles maintained their initial state of

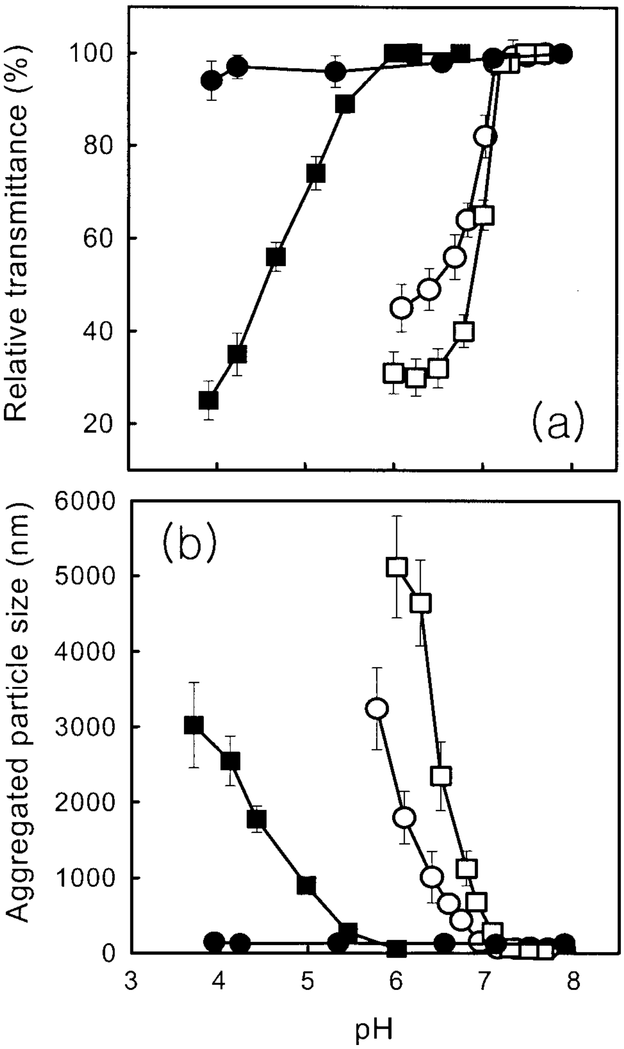

Fig. 3. Changes in turbidity (a) and particle size (b) of self-assembled hydrogel nanoparticles on decreasing pH. PA (●), coohPA (■), PA/SDM 1 (○) and 2 (□) nanoparticles.

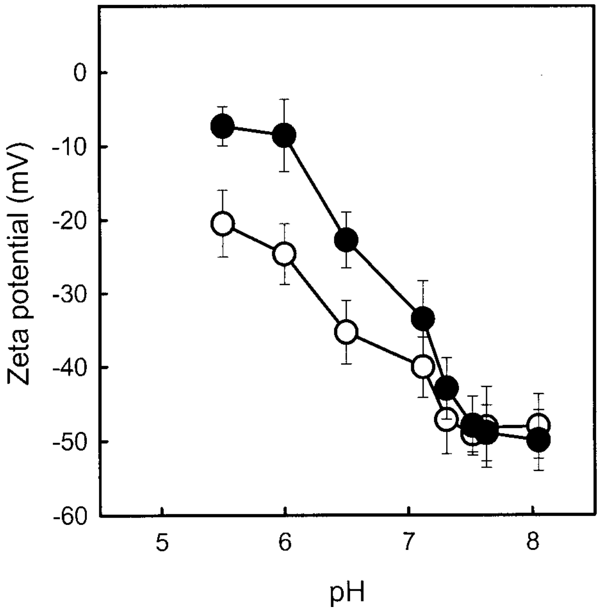

Fig. 4. Changes of zeta potential of PA/SDM hydrogel nanoparticles as a function of pH. PA/SDM 1 (○) and 2 (●).

colloidal suspension at pH 7.4 without any precipitation for at least 10 days.

pH-Dependent Aggregation of PA/SDM Nanoparticles

The aggregation behavior of the hydrogel nanoparticles in solution was studied by turbidity change [Fig. 3(a)] and particle size measurements [Fig. 3(b)] at various pHs. On decreasing the pH from 7.2 to 6.0, no turbidity change was observed for PA and coohPA, however, a significant change was observed for PA/SDM nanoparticles [Fig. 3(a)]. The transmittance of PA/SDM 2 nanoparticle solution drastically decreased from 100 at pH 7.2 to 38 at pH 6.7, indicating that turbidity transition occurred in 0.5 pH units. This change in turbidity was attributed to the aggregation of nanoparticles by hydrophobic interaction due to the deionization of surface located SDM. When PA/SDM hydrogel nanoparticles were prepared at pH 9.0, the outer shell was presumed to be composed of hydroxyl, carboxyl and SDM groups. Of these functional groups, SDM is the only group that can influence the particle surface charge by altering ionization/deionization in the pH range of 7.2 to 6.5. Moreover, the deionization of SDM could lead to pH-sensitive aggregation of the PA/SDM hydrogel nanoparticles because the SDM is characterized as hydrophobic in nature when unionized. A considerable change in turbidity and the slight shift of transition point to a higher pH at a higher content of SDM were also observed, and attributed to the increased hydrophobicity of the nanoparticles and the reduced charge-charge repulsion between particles caused by the reduced number of remaining carboxyl groups.

The aggregation behavior of PA/SDM nanoparticles can be demonstrated directly by measuring the particle size as a function of pH. The PA/SDM nanoparticles significantly associated on decreasing the solution pH from 7.2 to 6.0 as shown in Fig. 3(b). While the particle sizes of PA/SDM 1 and 2 were maintained below 70 nm above pH 7.4, however, the particle size grew to 450 and 1123 nm at pH 6.8, respectively. This result suggests that the PA/SDM nanoparticles may accumulate at tumor sites due to the synergic effect of aggregation behavior at tumor pH and the EPR effect.

As stated earlier, the aggregation of PA/SDM hydrogel nanoparticles is due to the deionization of ionizable groups on the surface. To observe the charge density and distribution of ionizable groups on the surface as a function of pH, the surface charge of the PA/SDM nanoparticles was measured using a zeta-potentiometer. The effect of pH on the zeta potential of the nanoparticles is shown in Fig. 4. It was found that the absolute value of zeta potentials of the PA/SDM 1 and 2 nanoparticles decreased below pH 7.4. In particular, the absolute value of zeta potential of PA/SDM 2 hydrogel nanoparticles decreased sharply from −48 mV to −8 mV on decreasing the pH from 7.4 to 6.0. However, in the case of PA/SDM 1 the magnitude of the change over the same pH range was lower than that of PA/SDM 2. It was noted that the surface properties of the PA/SDM 2 nanoparticles are influenced more by SDM than those of the PA/SDM 1 nanoparticles, because of the higher degree of substitution, and thus, is less influenced by the properties of the carboxyl group. Thus, the reduction of surface charge, that is, the formation of hydrophobic domains on the surface of the nanoparticles,

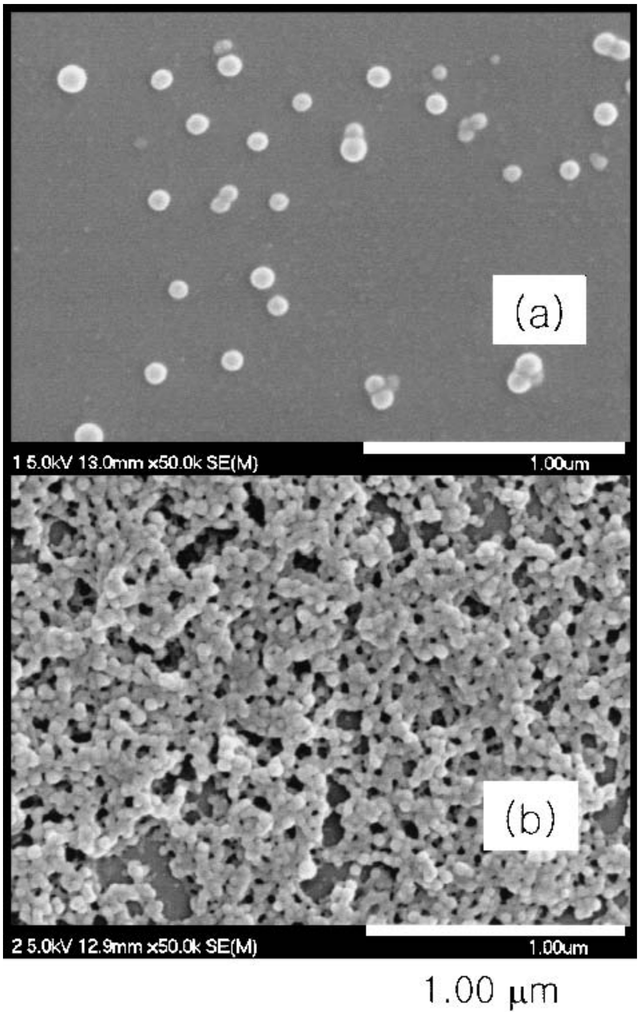

Fig. 5. Field-emission scanning electron microscopic (FE-SEM) photographs of PA/SDM 2 self-assembled hydrogel nanoparticles (scale bar = 1 μm) at pH 9.0 (a) and 6.4 (b).

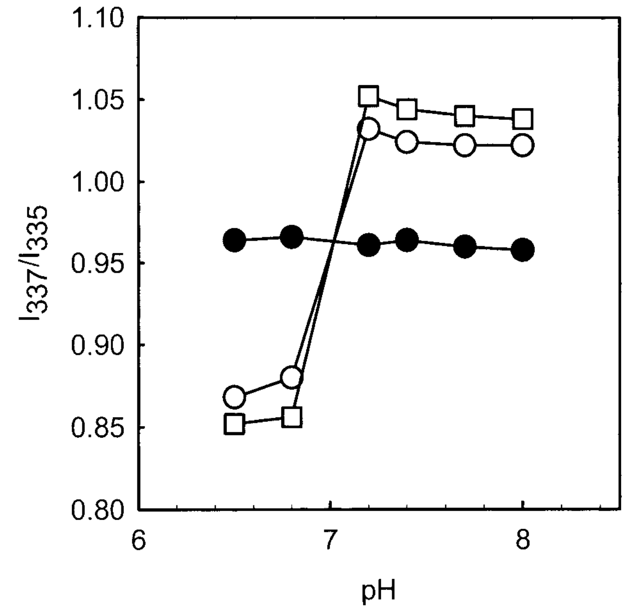

Fig. 6. A plot of the intensity ratio I_{337}/I_{335} from the excitation spectra vs. the pH of self-assemblies (0.05 g/L). coohPA (■), PA/SDM 1 (○) and 2 (□) nanoparticles.

caused by deionized SDM, leads to the aggregation by hydrophobic interaction of nanoparticles below pH 7.0.

On the other hand, ionized SDM groups on the surfaces of the nanoparticles surface cause repulsion between nanoparticles, which results in their improved stability observed above pH 7.4. This data also shows that although the pKa of the secondary amine in the SDM monomer is 6.1, that the transition pH is higher. This is explained by the fact that when monomers with ionizable groups are copolymerized or attached to a polymer, the pKa of ionizable groups usually shifts toward a higher pH range (21). This is because intervening water molecules cannot adequately provide the degree of hydration required to stabilize the charged form when the hydrophobic and chargeable groups are in close proximity.

Morphologies of PA/SDM Nanoparticles at Different pHs

The pH-sensitive behaviors of PA/SDM hydrogel nanoparticles were observed as morphology changes by FE-SEM. Each PA/SDM 2 nanoparticle size at pH 9.0 had well defined spherical particle of 50–90 nm and was well dispersed [Fig. 5(a)], which is in accord with the DLS results. However, at pH 6.4 each PA/SDM 2 nanoparticle size reduced to 20–30 nm and aggregated, while keeping a spherical shape [Fig. 5(b)]. This result indicates that at pH 6.4, this nanoparticle is compacted due to dehydration of the swollen shell.

pH-Induced Interior Structural Changes of PA/SDM Nanoparticles

To study the effect of pH on the structure of the PA/SDM nanoparticle interior, we monitored the micropolarity of pyrene (5). A nanoparticle solution (0.5 mL, pH 9.0) at a concentration of 1.0 mg/mL equilibrated with pyrene (6×10^{-7} moles) at 60°C for 12 h was diluted with 9.5 mL of PBS (ionic strength = 0.15 with varying pH).

Above pH 7.4, the total fluorescence intensity remained

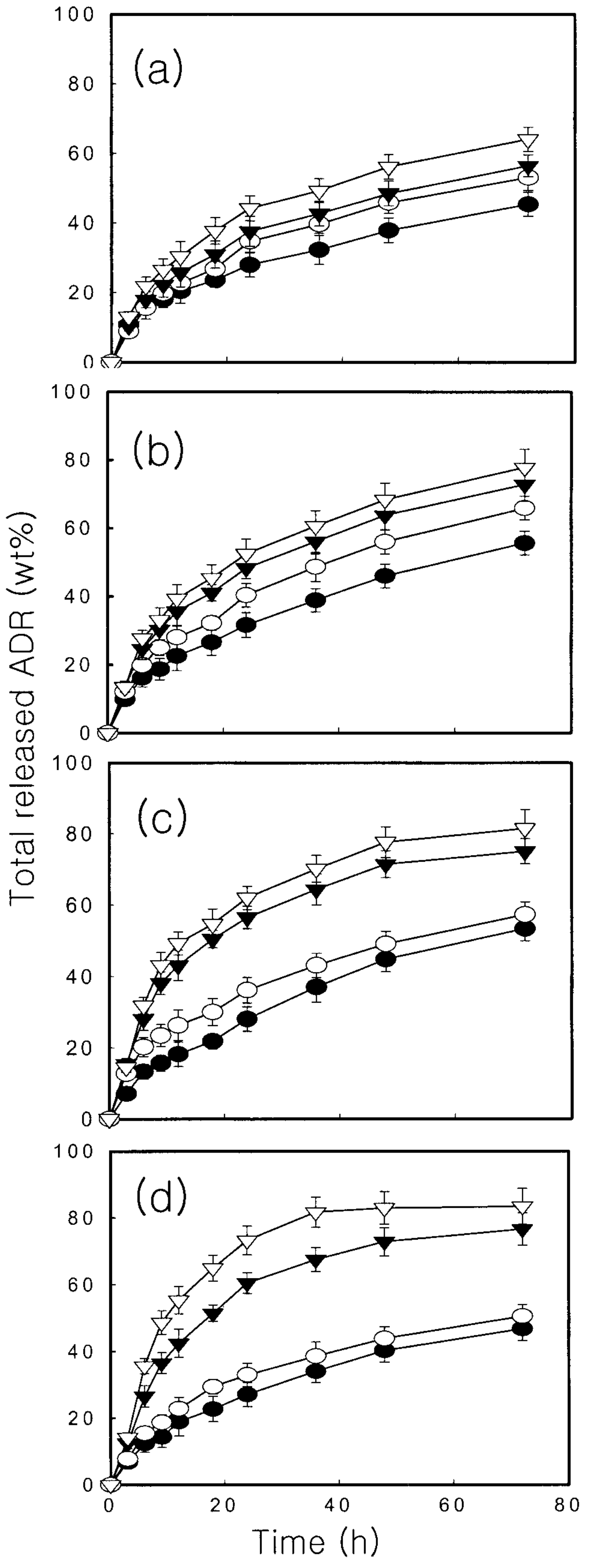

Fig. 7. ADR release kinetics from PA (a), coohPA (b), PA/SDM 1 (c) and PA/SDM 2 (d) self-assembled hydrogel nanoparticles loaded around physiological pH. pH 8.0 (●), 7.4 (○), 6.8 (▼) and 6.4 (▽).

unchanged and the (0,0) band appeared at 337 nm, however, the band intensity sharply decreased from pH 7.2 on decreasing pH and was shifted to 335 nm below pH 6.8, demonstrating that the pyrene molecules in nanoparticles were exposed to a more polar environment as the pH decreased (data not shown). To quantify the polarity around the pyrene molecules remained in nanoparticles, the pH effect on the intensity ratio (I_{337}/I_{335}, lower ratios indicate a more polar environment), of coohPA, PA/SDM 1 and 2 were measured and shown in Fig. 6. The coohPA nanoparticles did not show any change in micropolarity around pyrene over the tested pH range. In contrast, pyrene molecules in PA/SDM nanoparticles experienced a sharp increase in polarity at pH 6.8 and 6.4, while above pH 7.2 no further change in polarity was observed. In particular, at pH 7.2 the micropolarity of pyrene in PA/SDM nanoparticles was slightly lower than that at pH 7.4. This implies that on decreasing the pH from 7.4 to 7.2, the pyrene molecules in nanoparticles are associated with more hydrophobic groups in the interior of the nanoparticles.

Therefore, we assumed that the deionized SDM in the nanoparticles below pH 7.4 form new hydrophobic domains, which perturb the internal structure of the nanoparticles and lead to conformational changes and to the dehydration of the PA/SDM nanoparticles. Despite this microenvironmental change, the overall shape of the nanoparticles, although shrunken, remained spherical, as is shown in Fig. 5(b).

ADR Loading and Release

We selected ADR as a model because it has a broad spectrum of activity in human tumors, but is limited in use due to its non-selective toxicity. All hydrogel nanoparticles tested were successfully loaded with ADR, which indicated that ADR was physically incorporated and stabilized in the hydrophobic domains of the nanoparticles.

Figure 7 shows the kinetics of drug release from hydrogel nanoparticles loaded with ADR at various pHs (8.0, 7.4, 6.8, and 6.0). Although the ADR release patterns from PA and coohPA nanoparticles show a slight pH dependency; i.e., the amount of ADR released increased with decreasing medium pH, this may be the result of the pH-dependent solubility of ADR (a weak base, pKb = 8.22). However, at pH 6.8, the amounts of ADR released from both PA/SDM 1 (56%) and PA/SDM 2 (60%) nanoparticles in 24 h were drastically increased compared to that at pH 7.4 (33%).

In general, the release rate of a drug incorporated in a hydrophobic domain depends on the solubility and diffusivity of the drug. However, in the case of polymeric nanoparticles prepared from stimuli-sensitive amphiphilic polymers, the drug release rate can be rapidly altered by deformation of the inner core caused by external stimulation (5). Therefore, pH-accelerated ADR release from PA/SDM nanoparticles may be consistent with pH-induced structural change. The deionized SDM inner particle at a pH below 7.2 may form new hydrophobic interactions. This interaction may lead to interior-structural deformation and the dehydration of the PA/SDM nanoparticles, and result in conformational change, such as particle shrinkage. Furthermore, the aggregation of deionized SDM on the surface of PA/SDM nanoparticles may accelerate nanoparticle structural deformation, again influencing the drug release rate.

CONCLUSIONS

This study was undertaken to investigate hydrogel nanoparticles self-assembled from pullulan acetate-sulfadimethoxine conjugates (PA/SDM), which have potential use as an anti-cancer drug delivery system responsive to tumor extracellular pH. Nanoparticles formed at pH 9.0 by the diafiltration method were smaller than 70 nm in size and had a unimodal size distribution, indicating an optimum size for passive tumor targeting. The nanoparticles were proven to be stable on dilution and over 10 days at a fixed concentration of 1 g/L at pH 7.4 and room temperature. However, the particles shrank and aggregated at pH below 7.2 because of the deionizion of SDM. Moreover, the lower pH enhanced the release rate of the loaded adriamycin. Further optimization of the properties of these nanoparticles, and study of their interactions with tumor cells, may provide a more effective anti-cancer drug carrier with improved passive accumulation, and enhanced drug release at tumor pH_e.

ACKNOWLEDGMENTS

This work was financially supported by the Korean Organization of Science and Engineering Foundation through the Hyperstructured Organic Materials Research Center and BK21 program in Korea.

REFERENCES

1. H. Maeda, J. Wu, T. Sawa, Y. Matsumura, and K. Hori. Tumor vascular permeability and the EPR effect in macromolecular therapeutics: a review. *J. Control. Release* **65**:271–284 (2000).
2. D. C. Drummond, O. Meyer, K. Hong, D. B. Kirpotin, and D. Papahadjopoulos. Optimizing liposomes for delivery of chemotherapeutic agent to solid tumors. *Pharmacol. Rev.* **51**:691–743 (1999).
3. M. Yokoyama and T. Okano. Targetable drug carriers: present status and a future perspective. *Adv. Drug Deliv. Rev.* **21**:77–80 (1996).
4. G. Kong, R. D. Braun, and M. W. Dewhirst. Characterization of the effect of hyperthermia on nanoparticle extravasation from tumor vasculature. *Cancer Res.* **61**:3027–3032 (2001).
5. J. E. Chung, M. Yokoyama, and T. Okano. Inner core segment design for delivery control of thermo-responsive polymeric micelles. *J. Control. Release* **65**:93–103 (2000).
6. S. Cammas, K. Suzuki, C. Sone, Y. Sakurai, K. Kataoka, and T. Okano. Thermo-responsive polymer nanoparticles with a core-shell micelle structure as site-specific drug carriers. *J. Control. Release* **48**:157–164 (1997).
7. I. F. Tannock and D. Rotin. Acid pH in tumors and its potential for therapeutic exploitation. *Cancer Res.* **49**:4373–4384 (1989).
8. M. Stubbs, P. M. J. McSheehy, J. R. Griffiths, and C. L. Bashford. Causes and consequences of tumor acidity and implications for treatment. *Mol. Med. Today* **6**:15–19 (2000).
9. J. Conner, M. B. Yatvin, and L. Huang. pH-sensitive liposomes: Acid-induced liposomes fusion. *Proc. Natl. Acad. Sci. USA* **81**: 1715–1718 (1984).
10. M. Greidziak, A. A. Bogdanov, V. P. Torchilin, and J. Lasch. Destabilization of pH-sensitive liposomes in the presence of human erythrocyte ghosts. *J. Control. Release* **20**:219–230 (1992).
11. J. C. Leroux, E. Roux, D. L. Garrec, K. Hong, and D. C. Drummond. N-isopropylacrylamide copolymers for the preparation of pH-sensitive liposomes and polymeric micelles. *J. Control. Release* **72**:71–84 (2001).
12. D. C. Drummond, M. Zignani, and J. C. Leroux. Current status of pH-sensitive liposomes in drug delivery. *Prog. in Lipid Res.* **39**: 409–460 (2000).
13. M. Zignani, D. C. Drummond, O. Meyer, K. Hong, and J. C.

Leroux. *In vitro* characterization of a novel polymeric-based pH-sensitive liposome system. *Biochim. Biophys. Acta* **1463**:383–394 (2000).

14. O. Meyer, D. Papahadjopoulos, and J. C. Leroux. Copolymers of N-isopropylacrylamide can trigger pH sensitivity to stable liposomes. *FEBS Lett.* **421**:61–64 (1998).
15. J. Tailefer, M. C. Jones, N. Brasser, J. E. van Lier, and J. C. Leroux. Preperation and characterization of pH-responsive polymeric micelles for the delivery of photosensitizing anticancer drugs. *J. Pharm. Sci.* **89**:52–62 (2000).
16. K. Xi, Y. Tabata, K. Uno, M. Yoshimoto, T. Kishida, Y. Sokawa, and Y. Ikada. Liver targeting of interferon though pullulan conjugation. *Pharm. Res.* **13**:1846–1850 (1996).
17. T. Nishikawa, K. Akiyoshi, and J. Sunamoto. Macromolecular complexation between bovine serum albumin and self-assembled hydrogel nanoparticle of hydrophobized polysaccharide. *J. Am. Chem. Soc.* **118**:6110–6115 (1996).
18. E. E. Smissman. Sulfonamides and sulfones with antibacterial action. In C. O. Wilson, O. Gisvold, and R. F. Doerge (eds), *Textbook of organic medicinal and pharmaceutical chemistry.* J. B. Lippincott Co., Philadelphia, Pennsylvania, 1971 pp. 283–299.
19. S. Y. Park and Y. H. Bae. Novel pH-sensitive polymers containing sulfonamide groups. *Macromol. Rapid Commun.* **20**:269–273 (1999).
20. M. Yokoyama. Novel passive targeting drug delivery with polymeric micelles. In T. Okano (ed.), *Biorelated polymers and gels*. Academic Press, Tokyo, 1998 pp. 193–229.
21. D. W. Urry, S. Q. Peng, T. M. Parker, D. C. Gowda, and R. D. Harris. Relative significance of electrostatic and hydrophobic-induced pKa shifts in a model protein: the aspartic acid residue. *Angew. Chem. Int. Ed. Engl.* **32**:1440–1442 (1993).